THE JOURNAL OF BIOLOGICAL CHEMISTRY
Vol. 274, No. 26, Issue of June 25, pp. 18589–18596, 1999

Printed in U.S.A.

Formation of Fibrous Aggregates from a Non-native Intermediate: The Isolated P22 Tailspike β-Helix Domain*

(Received for publication, February 10, 1999, and in revised form, April 5, 1999)

Benjamin Schuler‡§, Reinhard Rachel¶, and Robert Seckler‖

From the ‡Institut für Biophysik und Physikalische Biochemie and the ¶Institut für Biochemie, Genetik und Mikrobiologie, Universität Regensburg, 93040 Regensburg, Germany and the ‖Physikalische Biochemie, Universität Potsdam, Im Biotechnologiepark, 14943 Luckenwalde, Germany

In the assembly pathway of the trimeric P22 tailspike protein, the protein conformation critical for the partitioning between productive folding and off-pathway aggregation is a monomeric folding intermediate. The central domain of tailspike, a large right-handed parallel β-helix, is essentially structured in this species. We used the isolated β-helix domain (Bhx), expressed with a hexahistidine tag, to investigate the mechanism of aggregation without the two terminal domains present in the complete protein. Although Bhx has been shown to fold reversibly at low ionic strength conditions, increased ionic strength induced aggregation with a maximum at urea concentrations corresponding to the midpoint of urea-induced folding transitions. According to size exclusion chromatography, aggregation appeared to proceed via a linear polymerization mechanism. Circular dichroism indicated a secondary structure content of the aggregates similar to that of the native state, but at the same time their tryptophan fluorescence was largely quenched. Microscopic analysis of the aggregates revealed a variety of morphologies; among others, fibrils with fine structure were observed that exhibited bright green birefringence if viewed under cross-polarized light after staining with Congo red. These observations, together with the effects of folding mutations on the aggregation process, indicate the involvement of a partially structured intermediate distinct from both unfolded and native Bhx.

Whereas some small single-domain proteins have been shown to fold without detectable intermediates (1–4), many larger, especially multidomain and oligomeric proteins are known to populate intermediates during their folding process, often leading to aggregation as a side reaction (5). Insoluble aggregates of normally well behaved proteins are characteristic of a variety of human disease states, including various forms of amyloidosis (6, 7) and the prion diseases (8). Protein aggregation is also a common problem encountered during the heterologous expression of proteins or their renaturation *in vitro* (9). Processes such as the formation of inclusion bodies or aggregation during refolding *in vitro* were commonly regarded as being driven by nonspecific, hydrophobic interactions between random coil or molten globule-like states of proteins. The formation of extracellular amyloid fibrils, on the other hand, has frequently been illustrated according to the sickle hemoglobin model, which invokes the alteration of surface properties of the native state of proteins as the reason for noncovalent polymerization. A growing body of evidence, however, suggests that protein aggregation in most cases occurs by mechanisms involving structured folding intermediates. Early studies, *e.g.* on tryptophanase (10), lactate dehydrogenase (11), and bovine growth hormone (12), had suggested a model involving structured folding intermediates, with domains or subdomains folded as they are in the native state but which undergo intermolecular rather than intramolecular interactions. This concept has meanwhile been well established for a series of other proteins, especially some of those known to be involved in human amyloid diseases such as transthyretin (13), immunoglobulin light chains (14), or lysozyme (15).

An important model protein used to study the kinetic partitioning between folding and aggregation is the tailspike of bacteriophage P22. Tailspike folding yields decrease dramatically with increasing temperature, with very similar dependences *in vivo* and *in vitro* (16–18). The temperature dependence is even more drastic for a type of mutants designated *temperature sensitive for folding* or *tsf*[1] (19, 20). These *tsf* mutations prevent the formation of the native trimer at high growth temperature, but once assembled at a lower permissive temperature, the mutant tailspike trimers have full biological activity at the restrictive temperature (21). *Tsf* mutations have been identified at more than 40 independent sites almost exclusively in the central β-helix domain (22–25), the main structural motif of tailspike (Fig. 1). A second class of mutations, isolated as *global suppressors* (*su*) of the *tsf* phenotype, have the opposite effect; they increase the yield of correctly assembled tailspikes at higher temperature, thus compensating for the effect of *tsf* mutations (26, 27).

Biophysical studies of tailspike folding *in vitro* confirmed that the *tsf* mutations affect tailspike folding by destabilizing thermolabile intermediates in the folding and assembly pathway and suggested that the *su* mutations stabilize such intermediates (28). A series of observations implied that the β-helix domain is largely structured in these intermediates (5, 29). Direct evidence for this hypothesis was obtained by expressing the central β-helix as an isolated domain (30) and investigating the effects of the *tsf* and *su* mutations on its stability (29). As opposed to the complete protein, unfolding of the isolated do-

* This work was supported by the Deutsche Forschungsgemeinschaft and the Fonds der Chemischen Industrie. The costs of publication of this article were defrayed in part by the payment of page charges. This article must therefore be hereby marked "*advertisement*" in accordance with 18 U.S.C. Section 1734 solely to indicate this fact.

The atomic coordinates and structure factors (codes 1LTK and 1TSP) have been deposited in the Protein Data Bank, Brookhaven National Laboratory, Upton, NY.

§ To whom correspondence should be addressed. Tel.: 49-941-943-3003; Fax: 49-941-943-2813; E-mail: ben.schuler@biologie.uni-regensburg.de.

[1] The abbreviations used are: *tsf*, temperature sensitive for folding (mutant); *su*, global suppressor (mutant); TSP, complete tailspike protein; GdmHCl, guanidinium hydrochloride; Bhx, isolated β-helix domain of the tailspike protein; TSPΔN, amino-terminally truncated TSP; SEC, size exclusion chromatography.

main is freely reversible in urea at low protein concentrations, low ionic strength, and low temperature, such that equilibrium data and thus a quantification of the effects of folding mutations on the thermodynamic stability can be obtained. The introduction of *tsf* mutations clearly destabilized, whereas *su* mutations stabilized the isolated domain. The differential effect of the four known *su* mutations on the stability of the isolated β-helix on the one hand, and on the native trimeric protein on the other, further suggested that the conformation of the isolated β-helix domain is close to that of the thermolabile intermediate populated during folding of the complete protein and responsible for kinetic partitioning between productive folding and aggregation (29).

The off-pathway reaction leading to the incorporation of tailspike chains into inclusion bodies has been studied *in vitro* by initiating refolding of the complete tailspike protein at intermediate denaturant concentrations at which a large fraction of the refolding chains can be induced to aggregate at temperatures as low as 20 °C (31, 32). Under these conditions, the association steps involved are irreversible and slow, allowing the electrophoretic separation of misassembly intermediates and their immunochemical analysis (32–34). Sequential multimeric species from dimers up to hexamers or heptamers were observed as misassembly intermediates, such that the misassembly reaction can be described as a linear polymerization process. The reaction is specific, in the sense that tailspike polypeptides do not form mixed aggregates with P22 coat protein chains or carbonic anhydrase when induced to aggregate simultaneously (33). This finding suggests that the aggregates, although reactive with anti-tailspike antibodies that do not recognize the native trimer, grow by incorporating tailspike chains in a specific, partly folded conformation rather than originating from unfolded chains.

Here we report on the investigation of the aggregation process of the isolated β-helix domain of tailspike. Reversible unfolding of the domain could be reached only under the optimized conditions described (30), but a drastic aggregation tendency had already been obvious from the handling of the protein during purification and storage, and reversible unfolding could not be attained at temperatures much above 10 °C or at high protein concentration. At low to medium protein concentration and low temperature, the aggregation process is slow enough to be analyzed by spectroscopic methods or size exclusion chromatography. The results suggest the involvement of a particularly aggregation-prone, structured equilibrium intermediate that can be stabilized by high ionic strength and that can lead to the formation of fibrous aggregates.

EXPERIMENTAL PROCEDURES

Materials—UV transparent plastic fluorescence cells (Kartell 4.5-ml PMMA cuvettes) were obtained from Semadeni (Ostermundingen, Switzerland). Ultrapure urea and guanidinium hydrochloride were purchased from ICN Biomedicals (Aurora, OH), and solutions containing urea were prepared fresh before use. Congo red was from Merck (Darmstadt, Germany). Denaturant concentrations were determined by refractive index measurements (35). The isolated β-helix domain was purified by immobilized metal ion affinity chromatography via a carboxyl-terminal hexahistidyl tag as described and stored at −70 °C (30).

Folding and Unfolding—Folding transitions were measured in a Perkin-Elmer MPF3 or a Spex FluoroMax spectrofluorometer with thermostatted cell holder using plastic fluorescence cuvettes or fused silica semimicro fluorescence cells at an excitation wavelength of 280 nm and an emission wavelength of 337 nm. CD measurements were made in an AVIV 62A-DS spectropolarimeter using calibrated fused silica semimicro fluorescence cells (path length, 4.2 mm; Hellma 104F-QS). For unfolding transitions, cold 50 mM sodium phosphate, pH 7.0, containing 0.5 M sodium chloride and 1 mM EDTA (Buffer A) was first added to a small volume of concentrated protein solution; then a cold concentrated urea solution of known molarity containing 50 mM sodium phosphate, pH 7.0, 0.5 M sodium chloride, and 1 mM EDTA was added to give a final volume of 1.2 ml (for measurements in plastic cuvettes) or 0.6 ml (for measurements in fused silica cuvettes) and an accurately known concentration of denaturant. For refolding transitions, urea solution was added first, the samples were incubated for at least 10 min, and refolding was initiated by rapid dilution with cold Buffer A. Mixing was carried out on ice if not indicated otherwise. For refolding kinetics, protein was denatured in Buffer A containing 6 M urea for at least 10 min. Refolding was initiated by rapid dilution to a final urea concentration of 2 M and a protein concentration of 100 μg/ml. Circular dichroism was recorded at 10 °C as described above.

Analytical Ultracentrifugation—Sedimentation equilibrium runs were performed in a Beckman Model E analytical ultracentrifuge using double-sector cells with a 12-mm optical path length and sample volumes of 360 μl (column height, 1.1 cm) at 18 °C and rotor speed between 3,000 and 12,000 rpm.

Light Scattering—Light scattering was measured in a Spex FluoroMax spectrofluorometer with thermostatted cell holder. Samples were stirred gently in silica semimicro fluorescence cells at 10 °C (Hellma 119.004F-QS), and the intensity of scattered light was measured using a wavelength of 360 nm. Protein denatured in Buffer A containing urea (see above) was rapidly mixed with Buffer A to a final urea concentration of 2 M, a protein concentration of 100 μg/ml, and a volume of 1.2 ml on ice, and then it was quickly transferred to a thermostatted cuvette. Control experiments performed under identical conditions with EDTA concentrations varying between 1 and 100 mM indicated that the aggregation observed was not the result of interaction of the hexahistidine tags, which is known to be mediated by divalent cations.[2]

Analytical Size Exclusion Chromatography—Separation of monomeric and aggregated protein was performed on a Superdex 200 HR 10/30 column (Amersham Pharmacia Biotech) at 5 °C and a flow rate of 30 ml/h. The reaction was initiated by rapidly diluting a solution of β-helix domain denatured in Buffer A containing 6 M urea with Buffer A to the urea concentration specified and a final protein concentration of 100 μg/ml on ice and then transferring it to a water bath thermostatted at 10 °C. For each chromatographic separation, 10-μl samples were taken from the thermostatted solutions after a given period of time, diluted to 100 μl with Buffer A at the respective urea concentration and 5 °C to attenuate further aggregation, and applied to the column equilibrated in the same buffer. Eluting protein was detected using a Merck/Hitachi F-1000 spectrofluorometer with flow cell at an excitation wavelength of 280 nm and an emission wavelength of 337 nm. Control experiments performed under identical conditions with solutions containing 1 mM dithioerythritol indicated that the aggregation observed was not the result of disulfide bond formation.

Microscopy—For light microscopy, an Olympus BX60 was used. Samples were taken directly from aggregation reactions at 2 M urea and 100 μg/ml protein as described above. For polarization microscopy, the same solutions were used, Congo red was added to a final concentration of 100 μM, and the samples were viewed in a Leitz Orthoplan polarization microscope with and without analyzer in search of the green birefringence known to be exhibited by amyloid-Congo red complexes (36, 37). For electron microscopy, samples were negatively stained with aqueous uranyl acetate (38) and analyzed in a Philips CM12 electron microscope equipped with a Gatan TV system 673 and a Tietz on-line control and processing unit (39).

RESULTS

Unfolding of the complete trimeric tailspike protein (TSP, Fig. 1) is known to be irreversible at elevated denaturant concentrations (40). This fact was evident from the hysteresis observed in guanidinium hydrochloride-induced folding transitions measured by tryptophan fluorescence (Fig. 2). Denaturation of the trimer takes place above 2 M GdmHCl, whereas refolding of monomers starting from unfolded chains is observed only at GdmHCl concentrations below about 0.6 M, and trimer reassembly is not detected above 0.2 M GdmHCl. Removal of the amino- and carboxyl-terminal domains of tailspike results in a reversibly folding monomeric protein, the isolated β-helix domain (Bhx), which trimerizes reversibly at high protein concentration with an association constant of $7 \cdot 10^9$ M^{-2} (30).

When folding transitions in GdmHCl were performed with

[2] A. Skerra, personal communication.

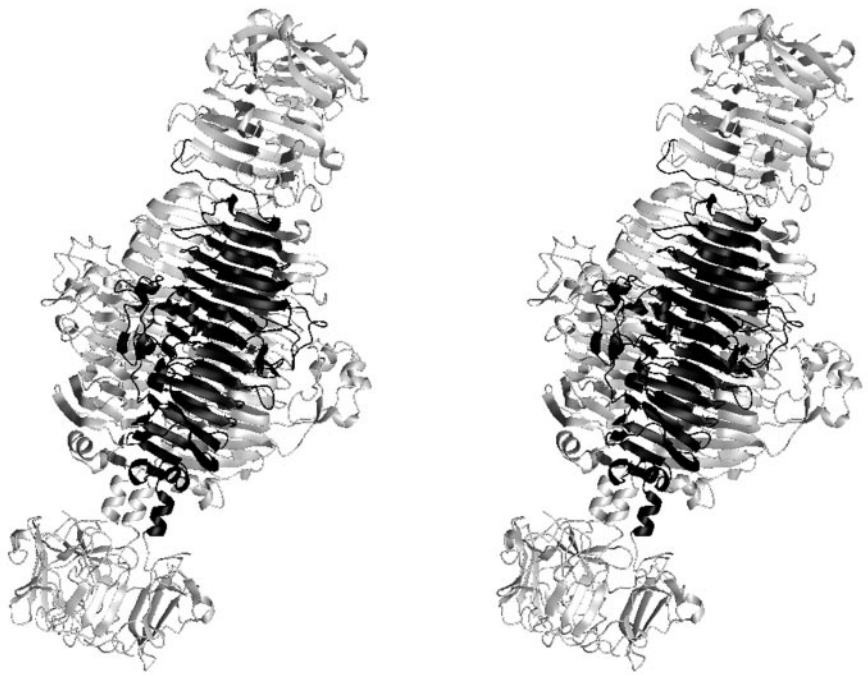

FIG. 1. **Crystal structure of the trimeric phage P22 tailspike protein.** A stereo ribbon representation of the complete tailspike protein is shown. The amino-terminal domain, for which the structure was solved separately (50), is located to the *lower left* and was docked manually to the structure of the amino-terminally shortened protein (51). The β-helix of one monomer (consisting of amino acids 108 to 544) corresponds to the region shown in *black* and was shown to adopt native-like structure if expressed as an isolated domain (30). This figure was constructed using the amino-terminal domain of tailspike (Protein Data Bank code 1TSP) and the carboxyl-terminal fragment (Protein Data Bank code 1LTK). The program MOLMOL was used (52).

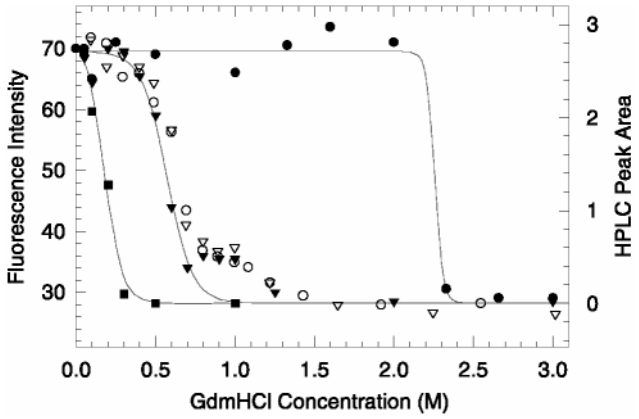

FIG. 2. **Folding transitions of TSP (*filled symbols*) and Bhx (*open symbols*) in GdmHCl at 10 μg/ml and 10 °C.** Unfolding transition (●), refolding transition (▼), and trimer reassembly (■) of TSP are taken from Ref. 40. Transitions for TSP were measured using fluorescence (excitation 280 nm, emission 335 nm) after an incubation time of 4 days, and trimer formation was analyzed by high pressure liquid chromatography (*HPLC*) after an incubation period of 7 days at 10 °C. Folding (▽) and unfolding (○) transitions for Bhx were prepared as described under "Experimental Procedures" using GdmHCl instead of urea, and tryptophan fluorescence was measured after an incubation time of 16 h. Note the resemblance of the refolding transition of TSP (▼) and the superimposable transitions of Bhx (▽, ○). The *lines* indicated are the spline curves shown in Ref. 40. The transitions measured by fluorescence are corrected for their post-transitional base-line slopes.

this fragment at low protein concentration, a striking resemblance was observed between the refolding transition of the complete protein leading to structured monomers and the superimposable unfolding and refolding transitions of the isolated β-helix domain (Fig. 2). Particularly remarkable was the coincidence of a plateau region at about 1 M GdmHCl that was found in both cases, identifying a separate state of conformation or association. Urea-induced folding transitions for Bhx, however, were observed to obey two-state behavior under otherwise identical conditions (29). Assuming that the decisive factor leading to this three-state behavior was the ionic character of GdmHCl, and to be able to directly compare the data to Bhx folding transitions measured before (29, 30), we attempted to simulate the conditions found in GdmHCl-induced denaturation by including sodium chloride at a concentration of 0.5 M in the solutions used for urea-induced unfolding.

To test the suitability of urea plus sodium chloride for generating three-state folding transitions, unfolding and refolding transitions were measured at a Bhx concentration of 200 μg/ml, which is sufficient for determining both tryptophan fluorescence and circular dichroism reliably (Fig. 3). The respective denaturation and renaturation curves were congruent, but a drastic difference in the relative CD and fluorescence signals was observed. Whereas the ellipticity at 220 nm showed an apparent two-state transition with slightly curved pre- and post-transition base lines, a clear plateau region was observed between 2 and 3.5 M urea when measuring tryptophan fluorescence. At a urea concentration of about 4 M, common transitions were detected with both signals, which were completely superimposable upon appropriate scaling of the data (Fig. 3, *inset*). This observation indicated the complete loss of secondary and tertiary structure at a urea concentration above 4.5 M, but it suggested that the secondary structure content was fairly constant up to this point. Although the congruence of unfolding and refolding transitions at first appeared to suggest reversibility of the folding transitions, no displacement of the two transition midpoints was found upon shifting the samples to lower temperature, which would be expected for an equilibrium process with a reaction enthalpy not equal to 0. On the other hand, a further increase of temperature lead to a broadening of the plateau, suggesting irreversible endothermic association as a possible process involved. To clarify the association state, analytical ultracentrifugation analysis of Bhx was attempted in Buffer A at a urea concentration of 2 M and 18 °C (data not shown). But the results unambiguously and repeatedly showed that a highly polydisperse population of molecules, including large, irreversibly formed aggregates, was present even at low protein concentrations, making an equilibrium analysis impossible.

To slow down the aggregation process and thus be able to follow its time course by the consecutive measurement of folding transitions, the protein concentration was lowered to 10

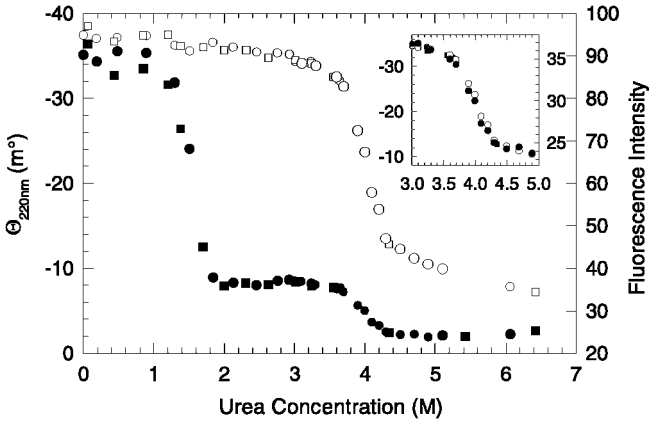

FIG. 3. **Bhx folding transitions in urea plus 0.5 M sodium chloride at 18 °C.** The protein concentration used was 200 μg/ml. Tryptophan fluorescence (●, ■) and CD (○, □) of the same samples were measured for both unfolding (●, ○) and refolding (■, □) after an incubation time of about 16 h. The *inset* shows a rescaled magnification of the signal change between 3 and 5 M urea to illustrate the congruence of the transitions observed in fluorescence and CD.

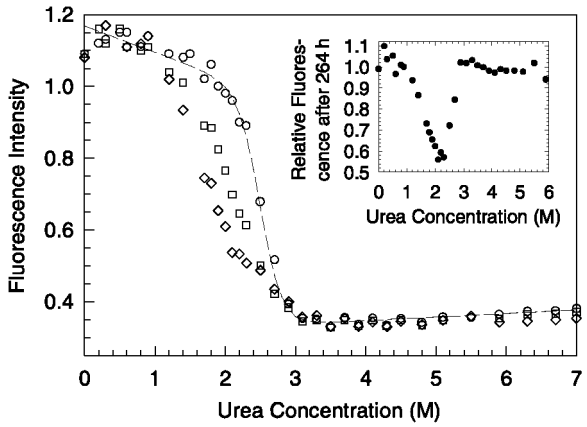

FIG. 4. **Change of fluorescence in Bhx folding transitions at high ionic strength with time.** Tryptophan fluorescence of the samples containing 10 μg/ml Bhx in Buffer A with varying concentrations of urea was measured 2 (○), 24, 72 (□), 168, and 264 h (◇) after the start of folding or unfolding at 10 °C (for clarity of presentation, the values for 24 and 168 h are not shown; a two-state fit from equilibrium measurements under identical conditions, but without sodium chloride (taken from Ref. 30), is shown by the *broken line* for comparison). The *inset* shows the values obtained by division of the fluorescence intensities measured after 264 h by those measured after 2 h, indicating that the strongest decrease of fluorescence occurs in the middle of the transition.

μg/ml and the temperature to 10 °C. Fluorescence of the samples was measured after t = 2, 24, 72, 168, and 264 h (Fig. 4). Again, unfolding and refolding curves were superimposable at all times, indicating that the presumptive aggregation process was slow compared with folding/unfolding under these conditions and, consequently, that the transition reflecting the *reversible* folding of the protein could be obtained from the data by extrapolation to t = 0. The apparent denaturation midpoint $c_{1/2}$ = 2.5 M of the folding transition resulting from such an extrapolation, which did not differ significantly from the data at t = 2 h, was identical to the value obtained from measurements without sodium chloride (29, 30). But contrary to what was found under low ionic strength conditions, a slow reduction of fluorescence intensity over time was observed at urea concentrations between about 1 and 3 M, such that a quantitative analysis of the data according to an equilibrium model for folding was not possible. Division of the fluorescence values obtained after an incubation time of 264 h by those obtained after 2 h yielded a peak of the relative fluorescence change between 2.0 and 2.4 M (Fig. 4, *inset*), indicating aggregation to be strongest at these urea concentrations.

A more detailed analysis of the aggregation process was performed using size exclusion chromatography (SEC) and fluorescence detection. A solution of Bhx in 6 M urea was diluted to different urea concentrations at t = 0. Samples were taken at times between 1 min and 24 h and applied to a SEC column, and the elution profiles were measured by tryptophan fluorescence. Apparently, equilibration of Bhx folding and unfolding was sufficiently slow relative to the duration of the separation such that monomeric folded and unfolded protein and aggregates could be clearly separated and resolved as distinct peaks in the elution profiles. Although a quantification of kinetics was complicated by the polydispersity of the aggregates and the decrease in tryptophan fluorescence upon both aggregation and unfolding (*cf.* Figs. 3 and 4), aggregation was obviously fastest at about 2.5 M urea. Representative elution profiles obtained after incubation of the samples at a protein concentration of 100 μg/ml for 1 h at 10 °C are shown in Fig. 5. Even at urea concentrations as low as 1 M, aggregation was observed, albeit at a much lower rate. Data for urea concentrations below 1 M could not be obtained because the interaction of the protein with the column matrix then drastically changed the elution profiles (data not shown). Especially at urea concentrations between 1 and 1.5 M, the formation of small oligomers could be well resolved. Their formation is irreversible on the time scale of at least 24 h as shown by reapplication of the corresponding eluted fractions onto the column (data not shown). The smallest oligomer observed elutes slightly earlier than amino-terminally shortened trimeric tailspike protein (TSPΔN, m = 180 kDa), which cannot be denatured by urea at pH 7 (17) and which was used as a reference at all urea concentrations investigated. But although the smallest oligomer observed almost co-eluted with trimeric TSPΔN, we assumed it to be the dimer for the following reason: if the logarithm of the degree of association were plotted *versus* the elution volume, a linear plot was obtained only under the assumption that the peaks observed corresponded to monomer, dimer, trimer, etc. or monomer, trimer, hexamer, etc. Extrapolation of these plots to the void volume of the column yielded a degree of oligomerization of about 13 for the first and about 65 for the second model (data not shown). Taking into account that the extrapolated exclusion limit of the column used was about $1.3 \cdot 10^6$ Da for globular proteins, the second model can be excluded, even if one assumes a globular shape of the aggregates formed. Generally, a migration of the averaged high molecular weight peak toward the void volume of the column was found during the time course of the reaction at all urea concentrations, even after almost all monomeric protein had been taken up, indicating further association of multimeric species. With increasing urea concentration, the formation of small oligomers appeared to be disfavored. Simultaneous with the appearance of multimer peaks, the area of the peaks corresponding to monomeric protein decreased with time.

The congruence of denaturation and renaturation transitions (Figs. 3 and 4) had already implied that the folding equilibrium was reached at all urea concentrations before aggregation started to occur to a detectable degree, *i.e.* that folding kinetics were much faster than the kinetics of aggregation. Folding kinetics under conditions identical to those used for SEC confirmed structure formation as measured by far-UV CD to be much faster than aggregation as measured by light scattering (data not shown) and SEC (*cf.* Fig. 5). Similar to TSP (40), about 75% of the total CD amplitude could not be resolved by manual mixing (dead time, 10 s), and even the use of rapid

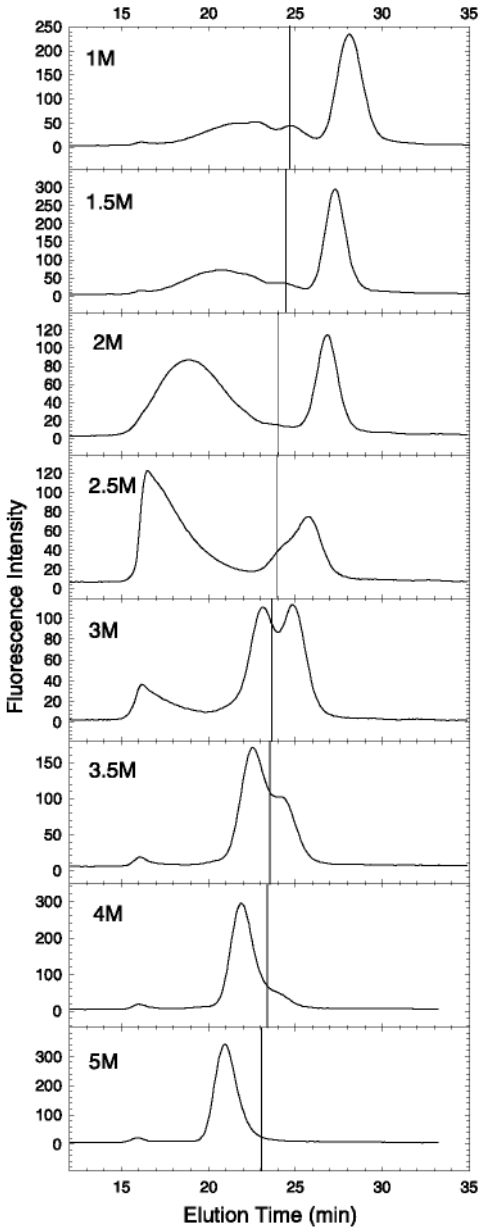

FIG. 5. **Size exclusion chromatography elution profiles after 1 h of incubation of 100 μg/ml Bhx at 10 °C.** Samples were taken from solutions of Bhx at different urea concentrations that were mixed starting from unfolded Bhx at $t = 0$. The samples were applied to a SEC column, and the elution profiles were determined by fluorescence detection. Maximum aggregation is observed at urea concentrations (indicated in the *top left* of each *panel*) corresponding to the middle of the folding transition measured by fluorescence at this temperature (*cf.* Fig. 4). Aggregation proceeds via formation of small oligomers, clearly separable on the column, yielding association states of higher order, corresponding to a migration of the peak arising from aggregates toward the void volume of the column. The elution times of trimeric tailspike protein lacking its amino-terminal domain under identical conditions are indicated by the *vertical lines* for comparison.

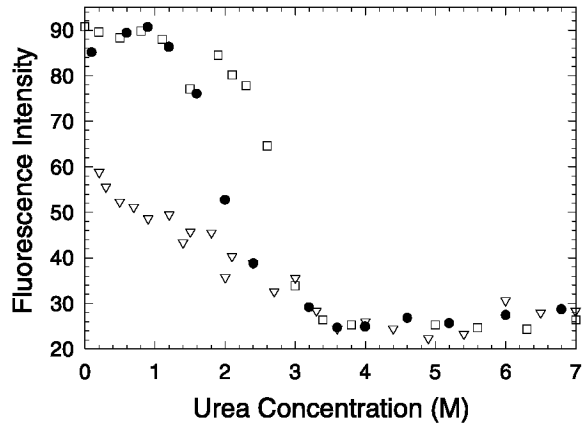

FIG. 6. **Aggregation tendency of folding mutants.** Samples of 10 μg/ml wild type (●), *su* mutant V331A (□), and *tsf* mutant G244R (△) were incubated at 18 °C for 16 h in Buffer A and then measured by fluorescence spectroscopy. The strongest deviation from apparent two-state behavior was observed for the *tsf* mutant, whereas the transition of the *su* mutant was virtually identical to the reversible curve found under low salt conditions.

mixing methods did not allow us to resolve this phase. The second phase of folding proceeds with a rate constant of about 1 min^{-1}. As the formation of secondary structure and tertiary structure are nonseparable processes in a parallel β-helix, the far-UV signal can be taken as indicative of both.

To assess the effect of folding mutations on the aggregation of Bhx, folding transitions of wild type, *su* mutant V331G, and *tsf* mutant G244R at a protein concentration of 10 μg/ml were incubated at 18 °C and measured by tryptophan fluorescence after 16 h (Fig. 6). The deviation from apparent two-state behavior was weakest for V331G and strongest for G244R, which exhibited a drastic decrease in fluorescence even at very low urea concentrations. A comparison with the equilibrium folding data obtained at low ionic strength (29) thus showed a clear correlation between the destabilization of the native β-helix domain and the influence on the aggregation tendency of the respective mutations.

To characterize the morphology of aggregates formed at 2 M urea, light microscopy, polarization microscopy, and electron microscopy were used. Even in a light microscope, large, elongated, laterally associated fibrillary aggregates containing fine structure were clearly detectable, with diameters ranging from about 0.05 μm for single fibrils to about 50 μm for lateral assemblies (Fig. 7*a*), although a large background of apparently amorphous aggregates of varying sizes was present. Additionally, flat, sheet-like and partially curled structures were observed (Fig. 7*b*). Electron microscopy of the negatively stained samples confirmed the morphologies found in the light microscopic analysis, including the presence of fine structure (Fig. 7*c*) and the background of irregular aggregates. Viewing samples stained with Congo red in a polarization microscope without analyzer showed all aggregates independent of morphology to bind Congo red, leading to an intense *red color* of the aggregates (Fig. 7*d*), which has been interpreted as an indication of β-structure making up the assemblies (41). Use of an analyzer with a polarization plane perpendicular to that of the polarizer revealed *bright green* birefringence for some of the aggregates described, especially those of large, fibrous morphology (Fig. 7*e*). For some of the thin fibrils without detectable fine structure, a faint birefringence was found, whereas neither the sheet-like structures nor the curled or amorphous aggregates exhibited detectable birefringence. Reasons for this could be either nonregular structure or insufficient thickness of the assemblies to polarize passing light to a detectable degree.

DISCUSSION

TSP and Bhx Aggregation—In the tailspike aggregation pathway, the critical species is the monomeric folding intermediate at the junction between productive folding and aggregation (16, 17). Several lines of evidence indicate that the β-helix is largely formed in this intermediate (5, 29). The effects of folding mutations on the stability of the isolated β-helix domain have shown that its structure is close to this intermediate, but

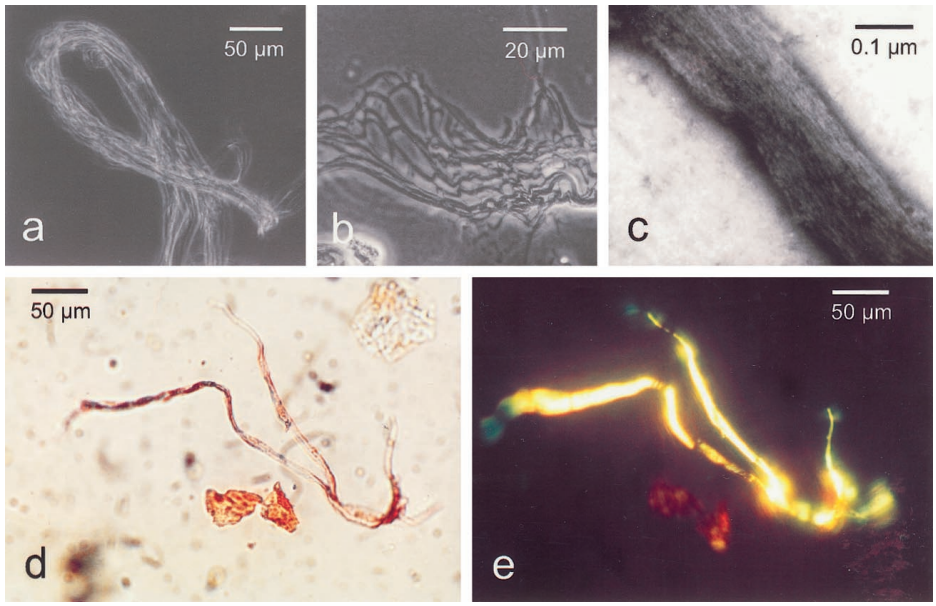

FIG. 7. **Microscopic analysis of Bhx aggregates.** Even in a light microscope, the characteristic features of the structures could be detected, *e.g.* multiple laterally aligned fibrils (*a*) and more extended, curly structures (*b*). Electron microscopy revealed fine structure even in very large fibrils (*c*) and confirmed a high background of smaller, amorphous aggregates without detectable fine structure. Addition of a 100 μM solution of Congo red led to the *red color* of all aggregates independent of their morphology (*d*), but only the fibrous aggregates exhibited *bright green* birefringence if viewed under cross-polarized light (*e*), indicating a high degree of regularity.

it is still native-like according to its spectroscopic and enzymatic properties (29, 30). The relevance of the β-helix domain for the folding of the complete tailspike is further supported by the similarities between TSP and Bhx in GdmHCl-induced folding transitions (Fig. 2). Even a similar plateau region was observed when measuring tryptophan fluorescence, indicating that a related phenomenon occurs with both proteins at about 1 M GdmHCl. For Bhx, a similar plateau, accompanied by a slow irreversible aggregation process, was found in urea-induced transitions if 0.5 M sodium chloride were added (Figs. 3–5). Maximum aggregation was observed at urea concentrations close to the folding transition midpoint prior to aggregation (Fig. 4), similar to what is known as the aggregation "trough" (10). Obviously, the increase in ionic strength caused by the additional salt is the reason for the loss of reversibility, as unfolding of Bhx is completely reversible at lower ionic strength (29, 30). Such an effect would be expected for metastable intermediates exposing hydrophobic surface that can give rise to intermolecular interactions (5), and a drastic influence of salt concentration on the formation of partially structured intermediates has been shown for transthyretin (13).

Aggregate Structure—A comparison of the data obtained from fluorescence-monitored folding transitions and SEC indicates that the maximum change in fluorescence intensity approximately coincides with maximum aggregation. The spectroscopic properties of the aggregates formed from Bhx at intermediate urea concentrations and high ionic strength indicate a secondary structure content similar to that of native protein but at the same time imply a drastically changed environment of at least some of the tryptophan residues present. Similar observations have been made for other proteins (5, 11), but in the case of a β-helix a drastic change of tertiary structure without simultaneous disruption of secondary structure is not plausible. Thus, possible explanations are (*a*) a rearrangement of the whole molecule to form a completely different β-structure in the aggregated state with a similar β-sheet content, (*b*) formation of an out-of-register β-helix with unfavorable packing, or (*c*) a local denaturation process, involving either the caudal fin domain, a tryptophan-rich 64 amino acid insertion between the third and fourth coil of the β-helix, or partial unfolding of terminal coils of the β-helix. In terms of aggregate structure, possibility *a* could be expected to lead to the formation of aggregates with the established cross-β structure (42), but possibilities *b* and *c* might cause fibril formation according to the recently proposed model, assuming an assembly of β-helical protofibrils for the formation of amyloid (43). An amyloid-like structure might be the basis of Bhx aggregates, at least in view of some of the morphologies found, their binding to Congo red, and the bright green birefringence under cross-polarized light typically used as a diagnostic tool to identify amyloid (36, 37). A significant shift of the point of maximum spectral difference in the Congo red binding assay in solution (41) was not observed, probably because of the high proportion of amorphous aggregates present. Growth of fibrils under optimized conditions might yield sufficiently homogeneous material to be suitable for x-ray diffraction, which could be used for a more detailed analysis of the Bhx aggregate structure. Remarkably, many of the fibrous structures observed here are curled or branched, and their diameters are larger by almost an order of magnitude than those of the typical amyloid fibrils observed so far (42).

Mechanism of Aggregation—The formation of aggregates obviously proceeds via a linear polymerization mechanism, because small oligomeric aggregation intermediates were observed by SEC, which could be assigned to dimers, trimers, and tetramers. Higher order multimers could not be resolved as separate peaks because of the decreasing differences in their elution volumes. This finding was in agreement with the detection of a linear series of oligomers formed from complete TSP chains under similar conditions by native gel electrophoresis (32). However, the SEC data not only suggest the formation of aggregates by a monomer addition pathway but also the association of multimeric species, corresponding to a cluster-cluster mode of polymerization (44), especially at later stages of the aggregation reaction. Again, this finding is in agreement with the observations made by Speed *et al*. (32). At higher urea concentration, however, no formation of small Bhx oligomers could be detected by SEC (Fig. 5), which is in contrast with observations on firefly luciferase (45) and carbonic anhydrase (46). For these proteins, the formation of large aggregates was prevented by high denaturant concentrations, whereas the formation of small multimers was still observed. To account for the absence of detectable amounts of small oligomers, it would be sufficient to assume that the rate of polymerization increases more steeply with increasing urea concentration than the rate of nucleation, which could be rationalized by the

higher cooperativity of the formation of large multimers compared with small ones. This notion would be equivalent to a nucleated polymerization mechanism at high urea concentrations, *i.e.* the rate-limiting formation of a higher order oligomer, which then polymerizes quickly to larger multimers by the addition of monomers or other small aggregates.

Evidence for an Aggregating Intermediate—Although the isolated β-helix domain of tailspike exhibits properties characteristic of the crucial folding intermediate at the switch between productive folding and aggregation of the complete tailspike (29), it still has to be regarded a native structure, because its enzymatic and spectroscopic properties are similar to those of TSP and, most importantly, because it exhibits a cooperative phase transition upon denaturant-induced unfolding (29, 30). In agreement with similar observations made for many other proteins (5, 13, 14), several lines of evidence indicate that an intermediate distinct from both the native and the unfolded state of Bhx is the species chiefly responsible for its aggregation. First, aggregation is fastest at medium concentrations of denaturant and is favored by high ionic strength, which has often been interpreted in terms of the presence of intermediates exposing hydrophobic surface (5, 9). Second, a clear correlation between the effects of folding mutations on the stability of the native state at low ionic strength (29) and the aggregation tendency under high salt conditions was observed here. Both observations exclude native state aggregation as the central process, although they do not rule out aggregation of unfolded protein (47, 48). But the ability of Bhx to associate to regular fibrillary structures is a persuasive indication of the regular structure of the monomers involved in this process, which suggests aggregation starting from the denatured state to be very improbable and leads us to conclude that a folding intermediate is the aggregating component. This conclusion is in agreement with the comparison of folding and aggregation kinetics. The formation of secondary structure starting from protein unfolded at high concentration of urea as monitored by CD is much faster than aggregation, suggesting that a fairly structured conformation is responsible for association. Finally, a contribution to the well ordered association process might arise from the comparatively high dipole moment of Bhx, which was calculated from the corresponding fragment of the TSP crystal structure to be about 80 Debye.

Structure of the Folding Intermediate—Nevertheless, the structure of this intermediate state so far remained elusive. Complicated by its short lifetime and strong aggregation tendency, clear differences between the native and the intermediate state could not be identified either by spectroscopy or 1-anilino-8-naphthalenesulfonate binding. Like the monomer or protrimer intermediate found during tailspike folding (17, 49), Bhx is highly susceptible to proteolysis. But again, preliminary trypsin digestion experiments did not reveal significantly different fractionation patterns upon analysis by SDS-polyacrylamide gel electrophoresis. However, in the high molecular weight range, similar band patterns and digestion kinetics were detected as for aggregates from complete TSP (32). Amino-terminal sequencing and estimation of the fragment size from polyacrylamide gels suggested preferred proteolysis at several sites in the carboxyl-terminal coils of the β-helix domain, particularly arginine residues 497, 502, and 507 (data not shown). Together with the strong dependence of elution volume of native Bhx on urea concentration compared with TSPΔN in SEC (Fig. 5), these findings might be taken to indicate a certain degree of flexibility and possibly partial unfolding of the terminal coils of the helix. Similarly, local unfolding of the caudal fin domain could lead to partially folded intermediates with increased urea binding tendency. This process does not necessarily have to result in a cooperative conformational transition as long as a central, cooperatively formed core of the β-helix domain remains intact. Furthermore, particularly in view of the different morphologies of aggregates formed, we cannot exclude the possibility of several conformationally distinct folding intermediates leading to aggregation of Bhx.

All in all, the isolated β-helix domain of tailspike seems to be a promising minimized model to investigate both the aggregation process of tailspike folding intermediates and the structure of aggregates formed from this large parallel β-helix. X-ray diffraction analysis of fibrils formed under optimized conditions might help to clarify structural changes involved in aggregate formation. In combination with a more detailed analysis of the monomeric precursor, possibly by site-directed mutagenesis, this analysis might lead to an elucidation of the conformations involved in tailspike misfolding and aggregation in general.

Acknowledgments—We thank Rainer Jaenicke for performing analytical ultracentrifugation runs, Gernot Endlicher for help with the polarization microscope, Christian Horn for access to the light microscope, and Thomas O. Baldwin for fruitful discussion. We also thank Margaret Sunde for helpful comments on the manuscript.

REFERENCES

1. Jackson, S. E., and Fersht, A. R. (1991) *Biochemistry* **30,** 10436–10443
2. Huang, G. S., and Oas, T. G. (1995) *Proc. Natl. Acad. Sci. U. S. A.* **92,** 6878–6882
3. Kragelund, B. B., Robinson, C. V., Knudsen, J., and Dobson, C. M. (1995) *Biochemistry* **34,** 7117–7224
4. Schindler, T., Herrler, M., Marahiel, M. A., and Schmid, F. X. (1995) *Nat. Struct. Biol.* **2,** 663–673
5. Jaenicke, R., and Seckler, R. (1997) *Adv. Protein Chem.* **50,** 1–59
6. Kelly, J. W. (1996) *Curr. Opin. Struct. Biol.* **6,** 11–17
7. Kelly, J. W. (1998) *Curr. Opin. Struct. Biol.* **8,** 101–106
8. Prusiner, S. B. (1997) *Science* **278,** 245–251
9. Mitraki, A., and King, J. (1989) *Bio/Technology* **7,** 690–697
10. London, J., Skrzynia, C., and Goldberg, M. E. (1974) *Eur. J. Biochem.* **47,** 409–415
11. Zettlmeissl, G., Rudolph, R., and Jaenicke, R. (1979) *Biochemistry* **18,** 5567–5571
12. Brems, D. N. (1988) *Biochemistry* **27,** 4541–4546
13. Kelly, J. W., Colon, W., Lai, Z., Lashuel, H. A., McCulloch, J., McCutchen, S. L., Miroy, G. J., and Peterson, S. A. (1997) *Adv. Protein Chem.* **50,** 161–181
14. Wetzel, R. (1997) *Adv. Protein Chem.* **50,** 243–264
15. Booth, D. R., Sunde, M., Bellotti, V., Robinson, C. V., Hutchinson, W. L., Fraser, P. E., Hawkins, P. N., Dobson, C. M., Radford, S. E., Blake, C. C., and Pepys, M. B. (1997) *Nature* **385,** 787–793
16. Haase-Pettingell, C. A., and King, J. (1988) *J. Biol. Chem.* **263,** 4977–4983
17. Danner, M., Fuchs, A., Miller, S., and Seckler, R. (1993) *Eur. J. Biochem.* **215,** 653–661
18. Seckler, R. (1997) in *Molecular Chaperones in the Life Cycle of Proteins* (Fink, A. L., and Goto, Y., eds) pp. 391–413, Marcel Dekker, New York
19. Smith, D. H., Berget, P. B., and King, J. (1980) *Genetics* **96,** 331–352
20. Betts, S. D., Haase-Pettingell, C., and King, J. (1997) *Adv. Protein Chem.* **50,** 243–264
21. Goldenberg, D. P., and King, J. (1981) *J. Mol. Biol.* **145,** 633–651
22. Yu, M.-H., and King, J. (1984) *Proc. Natl. Acad. Sci. U. S. A.* **81,** 6584–6588
23. Yu, M.-H., and King, J. (1988) *J. Biol. Chem.* **263,** 1424–1431
24. Villafane, R., and King, J. (1988) *J. Mol. Biol.* **204,** 607–619
25. Haase-Pettingell, C., and King, J. (1997) *J. Mol. Biol.* **267,** 88–102
26. Fane, B., Villafane, R., Mitraki, A., and King, J. (1991) *J. Biol. Chem.* **266,** 11640–11648
27. Mitraki, A., Fane, B., Haase-Pettingell, C., Sturtevant, J., and King, J. (1991) *Science* **253,** 54–58
28. Danner, M., and Seckler, R. (1993) *Protein Sci.* **2,** 1869–1881
29. Schuler, B., and Seckler, R. (1998) *J. Mol. Biol.* **281,** 227–234
30. Miller, S., Schuler, B., and Seckler, R. (1998) *Biochemistry* **37,** 9160–9168
31. Mitraki, A., Danner, M., King, J., and Seckler, R. (1993) *J. Biol. Chem.* **268,** 20071–20075
32. Speed, M. A., Wang, D. I., and King, J. (1995) *Protein Sci.* **4,** 900–908
33. Speed, M. A., Wang, D. I. C., and King, J. (1996) *Nat. Biotechnol.* **14,** 1283–1287
34. Speed, M. A., Moreshead, T., Wang, D. I. C., and King, J. (1997) *Protein Sci.* **6,** 99–108
35. Pace, C. N. (1986) *Methods Enzymol.* **131,** 266–280
36. Puchtler, H. F., Sweat, F., and Levine, M. (1962) *J. Histochem. Cytochem.* **10,** 355–364
37. Glenner, G. G., Eanes, E. D., Bladen, H. A., Linke, R. P., and Termine, J. D. (1974) *J. Histochem. Cytochem.* **22,** 1141–1158
38. Bremer, A., Henn, C., Engel, A., Baumeister, W., and Aebi, U. (1992) *Ultramicroscopy* **46,** 85–111
39. Rachel, R., Jakubowski, U., Tietz, H., Hegerl, R., and Baumeister, W. (1986) *Ultramicroscopy* **20,** 305–316

40. Fuchs, A., Seiderer, C., and Seckler, R. (1991) *Biochemistry* **30,** 6598–6604
41. Klunk, W. E., Pettegrew, J. W., and Abraham, D. J. (1989) *J. Histochem. Cytochem.* **37,** 1273–1281
42. Sunde, M., and Blake, C. (1997) *Adv. Prot. Chem.* **50,** 123–155
43. Lazo, N. D., and Downing, D. T. (1998) *Biochemistry* **37,** 1731–1735
44. Hemker, D. J., and Frank, C. W. (1990) *Macromolecules* **23,** 4404–4410
45. Herbst, R., Gast, K., and Seckler, R. (1998) *Biochemistry* **37,** 6586–6597
46. Cleland, J. L., and Wang, D. I. C. (1990) *Biochemistry* **29,** 1172–11078
47. De Young, L. R., Dill, K. A., and Fink, A. L. (1993) *Biochemistry* **32,** 3877–3886
48. Dill, K. A., and Stigter, D. (1995) *Adv. Protein Chem.* **46,** 59–104
49. Chen, B.-L., and King, J. (1991) *Biochemistry* **30,** 6260–6269
50. Steinbacher, S., Miller, S., Baxa, U., Budisa, N., Weintraub, A., Seckler, R., and Huber, R. (1997) *J. Mol. Biol.* **267,** 865–880
51. Steinbacher, S., Seckler, R., Miller, S., Steipe, B., Huber, R., and Reinemer, P. (1994) *Science* **265,** 383–386
52. Koradi, R., Billeter, M., and Wüthrich, K. (1996) *J. Mol. Graphics* **14,** 51–55